

Electrochemical behavior of Pd(II) and Rh(III) in [EMIm]NTf₂ ionic liquid*

GU Shuai (顾帅),¹ WANG Xin-Peng (王欣鹏),¹ WEI Yue-Zhou (韦悦周),^{1,†} and FANG Bai-Zeng (方百增)²

¹*School of Nuclear Science and Engineering, Shanghai 200240, China*

²*Department of Chemical & Biological Engineering, University of British Columbia, 2360 East Mall, Vancouver, British Columbia, V6T 1Z3, Canada*

(Received May 10, 2013; accepted in revised form June 12, 2014; published online December 20, 2014)

The electrochemical behavior of Pd(II) and Rh(III) in [EMIm]NTf₂ ionic liquid has been studied on Pt working electrodes at 298 K by cyclic voltammetry (CV), polarization curve and galvanostatic transient techniques. Cyclic voltammogram of Pd(II) in [EMIm]NTf₂ consists of two cathodic current peaks located at 1.37 V (E_{pc2}), corresponding to Pd²⁺/Pd⁺, and at 0.69 V (E_{pc1}) corresponding to Pd⁺/Pd. The transfer coefficient α was calculated by the Tafel extrapolation from the polarization curves to be 0.306, which is in agreement with the value reported in an aqueous solution system. For Rh(III) in [EMIm]NTf₂, a cathodic current peak (E_{pc}) was observed at -0.39 V, corresponding to Rh³⁺/Rh, and two oxidation peaks were observed at -0.13 V (E_{pa1}) and 0.37 V (E_{pa2}) during the reverse scan. A significantly negative shift in the cathodic peak potential was observed with the increase of the scan rate, indicating that the reduction of Pd(II) and Rh(III) on the Pt electrode involves kinetic complications. By using the galvanostatic transient technique, the diffusion coefficients of Pd(II) and Rh(III) in [EMIm]NTf₂ ionic liquid solution were found to be $\sim 10^{-7}$ cm²/s. The potential difference between the reduction of Pd(II) to Pd and the reduction of Rh(III) to Rh obtained from the CV curves of the Pd(II) and Rh(III) co-existing [EMIm]NTf₂ solution is found to be about 0.74 V, which makes it possible to electrodeposit Pd(II) and Rh(III) separately.

Keywords: Ionic liquids, Cyclic voltammogram, Palladium, Rhodium

DOI: [10.13538/j.1001-8042/nst.26.S10307](https://doi.org/10.13538/j.1001-8042/nst.26.S10307)

I. INTRODUCTION

Palladium and Rhodium are noble metals. Both of them play important roles in many industrial applications due to their unique physical and chemical properties, such as high catalytic activity [1–4]. To date, there has been a huge demand for rhodium, palladium, and their compounds in various industrial application areas. The abundance of rhodium and palladium in the Earth's crust are very low and only found in few countries. Therefore it is necessary to look for alternative sources of rhodium and palladium that is abundant and easily accessible. Meanwhile, spent fuels are composed of significant quantities of platinum group metals (PGMs). Most of the fission palladium and rhodium isotopes in the spent fuel are non-radioactive or very weakly radioactive [5, 6]. According to the report, by the year 2030 about 2500–3000 t of fission PGMs will be produced and only 7000 tonne of natural reserves will be left [5]. PGMs are rejected as waste during reprocessing of spent fuel by the PUREX process. In addition, PGMs increase the melting point of waste glass formed and tend to separate at a distinct phase during vitrification leading to a non-homogeneous glass matrix.

Direct electrodeposition of palladium from nitric acid [7] and hydrochloric acid [8, 9] have been studied before. However, it is not easy to obtain palladium films without hydrogen embrittlement by electrodeposition from a conventional aqueous plating bath since palladium has high catalytic activ-

ity towards hydrogen evolution and absorbs a great amount of hydrogen. Lately, room-temperature ionic liquids (RTILs) have drawn great attention and been studied in many fields [1, 10, 12]. RTILs have unique characteristics such as negligible vapor pressure, high chemical and thermal stability, acceptable intrinsic ionic conductivity, and a wide potential window. To avoid the influence of moisture in the air, a hydrophobic ionic liquid, [EMIm]NTf₂, was chosen for the study of the electrochemical behavior of Rh(III) and Pd(II).

II. EXPERIMENTAL SECTION

A. Materials and methods

[EMIm]NTf₂ was bought from the Lanzhou Institute of Chemical Physics, Chinese Academy of Sciences, and purified by recrystallization and vacuum drying at 353 K for 48 hours prior to use. Pd(NO₃)₂ (Sinopharm Chemical Reagent Co., Ltd. analytical pure, purity 99%) and RhCl₃ (J&K Scientific Ltd, analytical pure, purity 98%) were dissolved in [EMIm]NTf₂ in a container maintained at 353 K. The solution obtained after the complete dissolution was transferred into an electrochemical cell, which was maintained at 298 K in a water bath. The electrochemical experiments were carried out in a conventional three-electrode system. The working electrode was a platinum foil (apparent surface area = 1 cm²). A platinum wire electrode was used as the counter electrode. A reference electrode consisted of a silver wire immersed in 10 mmol/L AgCF₃SO₃/[EMIm]NTf₂ separated from the bulk solution by a porous glass. The potential of this reference electrode was measured by redox of ferrocene (Fc).

* Supported by the National Natural Science Foundation of China (Nos. 91026019 and 91126006)

† Corresponding author, yzwei@sjtu.edu.cn

Prior to each experiment, surface pretreatment of the working and counter electrodes were performed by hand polishing the electrode surface with 1.0, 0.3, 0.05 micro Gamma-Alpha alumina powder in a sequence to a mirror finish followed by immersing the electrode in 3 M HCl, acetone, methanol, and distilled water in an ultrasonic cleaner for 20 minutes, respectively, to remove any surface impurity. The electrolyte was deaerated by N_2 prior to each experiment.

B. Electrochemical measurements and software

All of the electrochemical measurements were conducted using an electrochemical workstation, CorrTestTM model C-S1350, equipped with electrochemical testing and analysis tools, Version 4.3 software.

III. RESULTS AND DISCUSSION

A. CV behavior of Fc^+/Fc in $[\text{EMIm}]\text{NTf}_2$

Cyclic voltammogram of Fc^+/Fc in $[\text{EMIm}]\text{NTf}_2$ obtained at the scan rate of 10 mV/s with the potential scan range from 1.10 V to 0.50 V is shown in Fig. 1. The electrolyte solution consisted of 2 mL of $[\text{EMIm}]\text{NTf}_2$ and 10 mmol/L Fc . The potential scan started from the OCP (Open Circuit Potential) to more positive potentials up to 1.10 V and then was reversed to 0.50 V. During the scan in the cathodic direction, the cathodic current density increased at a potential more negative than 0.90 V. The reduction peak was observed at ca. 0.74 V and after that the current starts to decrease due to the decreased Fc^+ concentration on the surface. During the reverse scan, the anodic peak was recognized at ca. 0.82 V, which is related to the oxidation of Fc to Fc^+ . It is clear that the Fc^+/Fc is a simple single-step one-electron-transfer reaction. The fact that the ratio of i_{pc}/i_{pa} approaches 1 and $E_{pc} - E_{pa} = 0.08$ V in Fig. 1 imply that the reaction of Fc^+/Fc in $[\text{EMIm}]\text{NTf}_2$ is a reversible reaction. The formula $E^f = (E_{pa} + E_{pc})/2$ allows for the calculation of the formal potential (E^f) of the process in Fig. 1, which is calculated to be $(0.82 + 0.74)/2 = 0.78$ V. Taking the fact that the Fc^+/Fc couple $E^\circ = 0.40$ V vs. NHE into consideration we can calculate the potential of the reference electrode is -0.38 V vs. NHE. All electrode potentials reported in this work are referred to the potential of the reference electrode.

B. Electrochemical behavior of Pd(II) or Rh(III) in $[\text{EMIm}]\text{NTf}_2$

Figure 2 shows the CV plot of platinum electrodes in the $[\text{EMIm}]\text{NTf}_2$ ionic liquids solution containing 5 mM PdCl_2 at the scan rate of 15 mV/s with the potential scan starting at 2.10 V to 0.12 V. A cathodic current peak (E_{pc2}) was observed at ca. 1.37 V and the other cathodic current peak (E_{pc1}) was observed at 0.69 V which can be explained by Eqs. (1), (2) and (3). During the reverse scan two oxidation

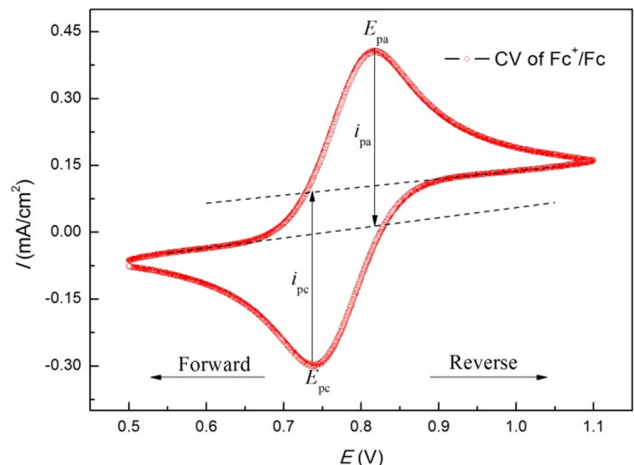


Fig. 1. (Color online) Cyclic voltammogram of the Fc^+/Fc couple in $[\text{EMIm}]\text{NTf}_2$ at 10 mV/s.

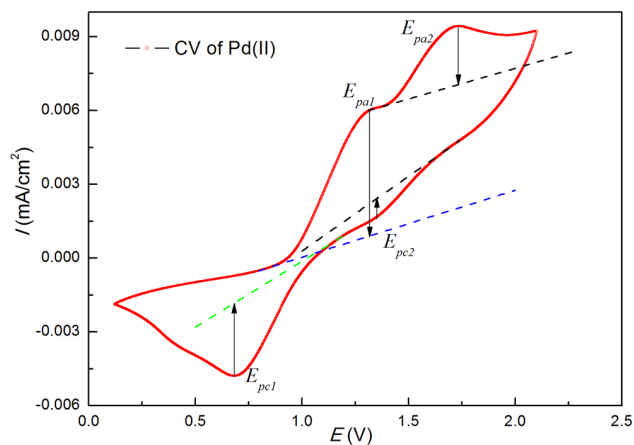
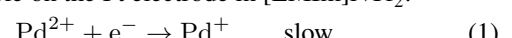


Fig. 2. (Color online) Cyclic voltammogram of 5 mM Pd(II) in $[\text{EMIm}]\text{NTf}_2$ obtained at Pt electrode at 15 mV/s.

peaks are observed at 1.33 V (E_{pa1}) and 1.72 V (E_{pa2}). The reduction of Pd(II) in an aqueous solution was reported to be a two-step electron transfer process [13, 14], as described by the Eqs. (1) and (2). The slower step (Eq. (1)) may lead to the accumulation of Pd(I) at the electrode surface when the potential is negative enough for $\text{Pd(II)}/\text{Pd(I)}$ but not negative enough for the $\text{Pd(I)}/\text{Pd}$ couple, resulting in a decrease of the current. This can explain the appearance of the peak (a) when $E_{pc2} = 1.37$ V. With further decrease of the potential, the absolute value of the current becomes much larger. The peak current at 0.69 V is likely attributed to the three electrode processes, as described by the Eqs. (1), (2), and (3). Namely, E_{pc2} and E_{pa2} are attributed to the redox process of the $\text{Pd(II)}/\text{Pd(I)}$ couple, while E_{pc1} and E_{pa1} correspond to the redox process of the $\text{Pd(I)}/\text{Pd}$ couple. The difference between E_{pc2} and E_{pa2} is calculated to be -0.35 V and the difference between E_{pc1} and E_{pa1} is -0.64 V, which indicate that the redox processes of the $\text{Pd(II)}/\text{Pd(I)}$ and $\text{Pd(I)}/\text{Pd}$ couples are both irreversible on the Pt electrode in $[\text{EMIm}]\text{NTf}_2$.



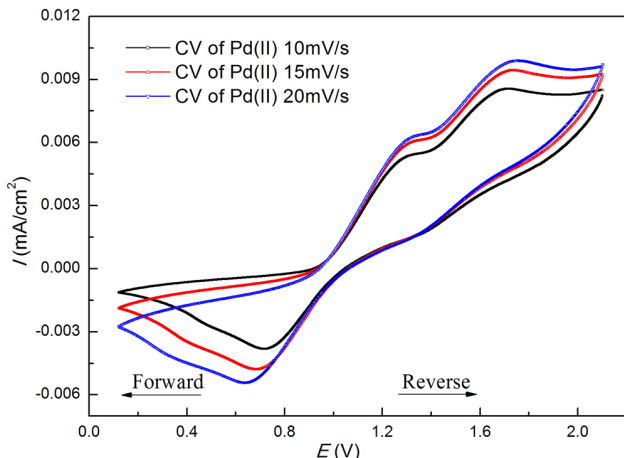
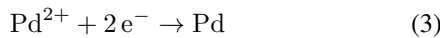


Fig. 3. (Color online) Cyclic voltammogram of 5 mM Pd(II) in [EMIm]NTf₂ with different scan rates.



A comparison of cyclic voltammograms of Pd(II) in [EMIm]NTf₂ at different scan rates is shown in Fig. 3. The cathodic peak current increases and the cathodic peak potential (E_{pc1} and E_{pc2}) shifts negatively with the increase of scan rate. This indicates that the reduction of Pd(II) at the Pt electrode is irreversible, which is in agreement with the conclusion derived from the CV plot obtained at 15 mV/s.

Figure 4 shows the polarization curves and the derived Tafel plots of the platinum electrode in the [EMIm]NTf₂ solution, containing 5 mM Pd(NO₃)₂ at the scan rate of 10 mV/s. At the initial cathodic potentials there is a linear relationship between the $\lg I$ and E , corresponding to the charge transfer limitation. As seen in Fig. 3, the equilibrium potential is located in the area of the one-electron transfer process, and thus the electron number transferred in this potential range is $n = 1$. According to the Tafel extrapolation method [15], the exchange current density, i^0 , is estimated to be 8.51×10^{-8} mA/cm² and the charge transfer coefficient, $\alpha = 0.306$, which is a little smaller but comparable to the value reported in an aqueous solution [16].

Figure 5 shows the CV plot of the platinum electrode in [EMIm]NTf₂ ionic liquid solution containing 5 mM RhCl₃ at the scan rate of 15 mV/s with the potential scan starting from 0.90 V to -0.70 V. A cathodic current peak (E_{pc}) was observed at -0.39 V, which is due to the reduction of Rh(III). During the reverse scan two oxidation peaks were observed at -0.13 V (E_{pa1}) and 0.37 V (E_{pa2}). These indicate that Rh(III) in [EMIm]NTf₂ ionic liquid undergoes an irreversible single step three electron transfer at the Pt electrode. The value (i.e., ca. 175 mV) of $|E_{pc} - E_{pc/2}|$ is much larger than that (i.e., 18.8 mV at 298 K) required [17] for a reversible process indicating that the reduction of Rh(III) in [EMIm]NTf₂ at the Pt electrode is not only controlled by diffusion, but also charge transfer kinetics.

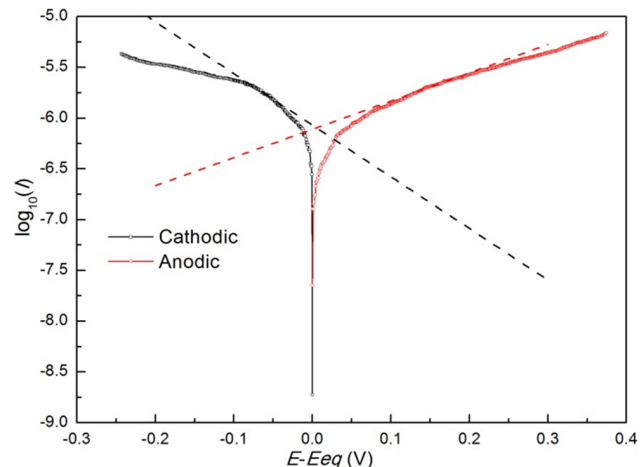


Fig. 4. (Color online) Polarization curves (solid line) and the derived Tafel plots of platinum electrode (dashed line) in the study solution.

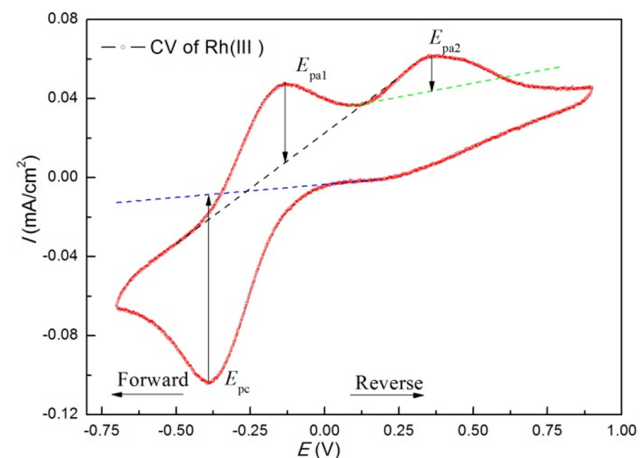


Fig. 5. (Color online) Cyclic voltammogram of 5 mM Rh(III) in [EMIm]NTf₂ (solid red line) obtained at 15 mV/s and the baseline of the platform (dashed line).

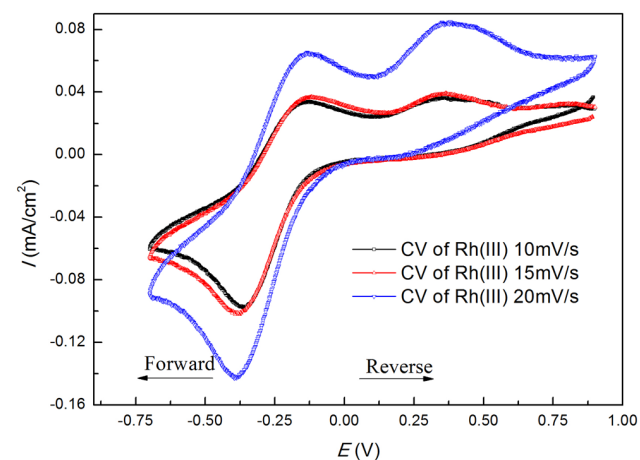


Fig. 6. (Color online) Cyclic voltammograms of 5 mM Rh(III) in [EMIm]NTf₂ obtained under different scan rates.

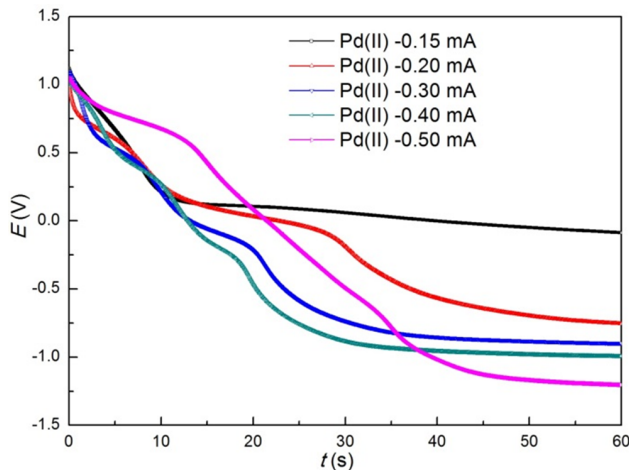


Fig. 7. (Color online) Chronopotentiograms of a Pt electrode in 5 mM Pd(II) in [EMIm]NTf₂ recorded at various current densities.

A comparison of cyclic voltammograms of Rh(III) in [EMIm]NTf₂ at different scan rates is shown in Fig. 6. The cathodic peak current increases and the cathodic peak potential E_{pc} shifts negatively with the increase in the scan rate, also indicating that the reduction of Rh(III) at the Pt electrode is irreversible.

Figures 7 and 8 show the chronopotentiograms of the Pt electrode in 5 mM Pd(II)/Rh(III) in [EMIm]NTf₂ ionic liquid solution recorded at different applied current densities. The plateau potential shifts negatively as the current density increases, which is a particular behavior of the irreversible electrode reaction. By measuring the transition time, τ , of each chronopotentiogram, we can calculate the diffusion coefficient of Pd(II)/Rh(III) in [EMIm]NTf₂ ionic liquid solution according to the sand equation:

$$\frac{I\tau^{1/2}}{C_0} = \frac{nF}{2} \sqrt{\pi D}, \quad (4)$$

where I is the current density, C_0 the bulk concentration of Pd(II) or Rh(III), n the number of electrons, and F is the Faraday constant. The diffusion coefficient of Pd(II) is calculated as 1.71×10^{-7} cm²/s and the diffusion coefficient of Rh(III) is calculated as 1.57×10^{-7} cm²/s.

C. Electrochemical behavior of Pd(II) and Rh(III) in [EMIm]NTf₂

As we mentioned above, both Pd(II) and Rh(III) are noble metals produced as fission products. The redox behavior of Pd(II) co-existing with Rh(III) was investigated by CV measurements. Fig. 9 shows the cyclic voltammogram of 5 mM Pd(II), 5 mM Rh(III), and 10 mM Fc⁺/Fc couple in [EMIm]NTf₂ recorded at the Pt electrode at 298 K at a scan rate of 15 mV/s with the potential scan starting from 2.00 V to -1 V. A cathodic current peak (marked as a) was observed at $E_{pc1} = 0.73$ V and the other cathodic current peak (marked as c) was observed at $E_{pc2} = -0.45$ V. During the reverse

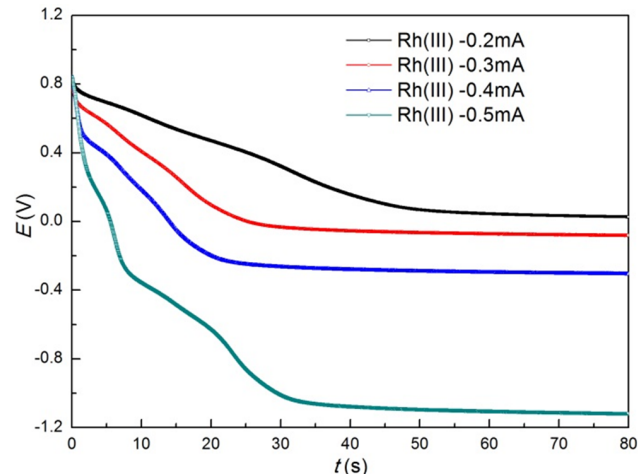


Fig. 8. (Color online) Chronopotentiograms of a Pt electrode in 5 mM Rh(III) in [EMIm]NTf₂ recorded at various current densities.

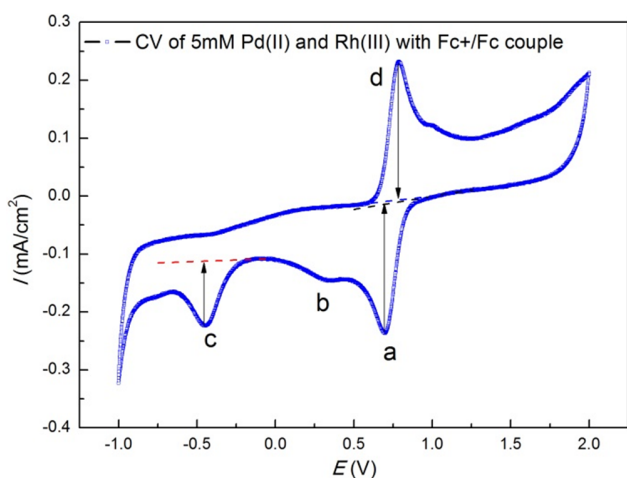


Fig. 9. (Color online) Cyclic voltammogram of 5 mM Pd(II), 5 mM Rh(III) and 10 mM Fc⁺/Fc couple in [EMIm]NTf₂ recorded at 15 mV/s.

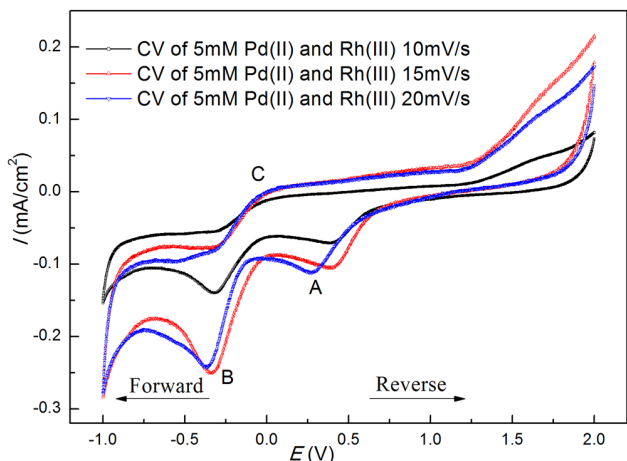


Fig. 10. (Color online) Cyclic voltammogram of 5 mM Pd(II) and 5 mM Rh(III) in [EMIm]NTf₂ recorded at various scan rates.

scan only one oxidation peak (marked as d) was observed at 0.81 V (E_{pa1}). According to Figs. 1 and 9 we can draw a safe conclusion that the peaks a and d are the redox process of the Fc^+/Fc couple, which proves the excellent reproducible property of the reference electrode. Fig. 10 shows the cyclic voltammograms of 5 mM Pd(II) and 5 mM Rh(III) in [EMIIm]NTf₂ recorded at the Pt electrode at 298 K with different scan rates. A cathodic current peak A (E_{pc1}) was observed at ca. 0.25–0.35 V, which is attributed to the reduction of Pd(II). This peak was also observed in Fig. 9 at peak b, which was overlapped by the current of the Fc^+/Fc couple. The other cathodic current, peak B (E_{pc2}), was observed at ca. –0.30 V which is due to the reduction of Rh(III). During the reverse scan, only one oxidation, peak C, was observed. The potential difference between the peaks A and B is about 0.74 V which makes it possible to electrodeposit Pd(II) and Rh(III) separately in [EMIIm]NTf₂ ionic liquid solution.

IV. CONCLUSION

The electrochemical behavior of Pd(II) and Rh(III) in [EMIIm]NTf₂ was studied by cyclic voltammetry, polariza-

tion curve, and chronopotentiometry measurements at the Pt electrode at 298 K. Two cathodic peaks were observed for the first time in 5 mM Pd(II)/[EMIIm]NTf₂ ionic liquid solution. The peak at 1.37 V (E_{pc2}) is attributed to the electrode process as described in Eq. (1) and the one at 0.69 V (E_{pc1}) corresponds to the process shown in Eqs. (1), (2), and (3). Based on this assumption the transfer coefficient, α , was calculated by the Tafel curve to be 0.306, which is in agreement with the value reported in an aqueous solution. A cathodic current peak (E_{pc}) was observed at –0.39 V, which is due to the reduction of Rh(III). During the reverse scan two oxidation peaks were observed at –0.13 V (E_{pa1}) and 0.37 V (E_{pa2}) in 5 mM Rh(III)/[EMIIm]NTf₂ ionic liquids solution. A significant negative shift in the cathodic peak potential was observed with the increase of scan rate, indicating that the reduction of Pd(II) and Rh(III) at the Pt electrode involve kinetic complication. The diffusion coefficient of Pd(II) and Rh(III) in [EMIIm]NTf₂ ionic liquid solution were found to be ca. 10^{-7} cm²/s, which is in accordance with the diffusion coefficient under similar conditions. The investigation of the redox behavior of Pd(II) co-existing with Rh(III) by cyclic voltammetry reveals a cathodic peak potential difference of ca. 0.74 V, implying that it is possible to electrodeposit Pd(II) and Rh(III) separately in [EMIIm]NTf₂ ionic liquid solution.

- [1] Miao F J and Tao B R. Methanol and ethanol electrooxidation at 3D ordered silicon microchannel plates electrode modified with nickel–palladium nanoparticles in alkaline. *Electrochim Acta*, 2011, **56**: 6709–6714. DOI: [10.1016/j.hydromet.2009.05.020](https://doi.org/10.1016/j.hydromet.2009.05.020)
- [2] Kazemi R and Kiani A. Deposition of palladium sub-monolayer on nanoporous gold film and investigation of its performance for the methanol electrooxidation reaction. *Int J Hydrogen Energy*, 2012, **37**: 4098–4106. DOI: [10.1016/j.ijhydene.2011.11.147](https://doi.org/10.1016/j.ijhydene.2011.11.147)
- [3] Gong T J, Cheng W M, Su W, et al. Synthesis of indoles through Rh(III)-catalyzed C–H cross-coupling with allyl carbonates. *Tetrahedron Lett*, 2014, **55**: 1859–1862. DOI: [10.1016/j.tetlet.2013.11.065](https://doi.org/10.1016/j.tetlet.2013.11.065)
- [4] Roy P S, Park N K, Kim K. Metal foam-supported Pd–Rh catalyst for steam methane reforming and its application to SOFC fuel processing. *Int J Hydrogen Energy*, 2014, **39**(9): 4299–4310. DOI: [10.1016/j.ijhydene.2014.01.004](https://doi.org/10.1016/j.ijhydene.2014.01.004)
- [5] Ache H J, Baetsle L H, Bush R P, et al. IAEA-TECDOC-308: Feasibility of separation and utilization of ruthenium, rhodium and palladium from high level waste. IAEA, Vienna, 1989.
- [6] Kolarik Z and Renard E V. Recovery of Value Fission Platinoids from Spent Nuclear Fuel. *Platinum Met Rev*, 2003, **47**: 74–87.
- [7] Jayakumar M, Venkatesan K A, Srinivasan T G, et al. Studies on the feasibility of electrochemical recovery of palladium from high-level liquid waste. *Electrochim Acta*, 2009, **54**: 1083–1088. DOI: [10.1016/j.electacta.2008.08.034](https://doi.org/10.1016/j.electacta.2008.08.034)
- [8] Kibler L A, Kleinert M, Randler R, et al. Initial stages of Pd deposition on Au(hkl) Part I: Pd on Au(111). *Surf Sci*, 1999, **443**: 19–30. DOI: [10.1016/S0039-6028\(99\)00968-1](https://doi.org/10.1016/S0039-6028(99)00968-1)
- [9] Gu S, Wang X P, Wei Y Z, et al. Mechanism for nucleation and growth of electrochemical deposition of palladium(II) on a platinum electrode in hydrochloric acid solution. *Sci China Chem*, 2014, **57**: 755–762. DOI: [10.1007/s11426-013-5026-2](https://doi.org/10.1007/s11426-013-5026-2)
- [10] Vasudeva Rao P R, Venkatesan K A, Srinivasan T G. Studies on applications of room temperature ionic liquids. *Prog Nucl Energy*, 2008, **50**(2–6): 449–455. DOI: [10.1016/j.pnucene.2007.11.079](https://doi.org/10.1016/j.pnucene.2007.11.079)
- [11] Galiński M, Lewandowski A, Stepienak I. Ionic liquids as electrolytes. *Electrochim Acta*, 2006, **51**: 5567–5580. DOI: [10.1016/j.electacta.2006.03.016](https://doi.org/10.1016/j.electacta.2006.03.016)
- [12] Jayakumar M, Venkatesan K A, Srinivasan T G. Electrochemical behavior of fission palladium in 1-butyl-3-methylimidazolium chloride. *Electrochim Acta*, 2007, **52**: 7121–7127. DOI: [10.1016/j.electacta.2007.05.049](https://doi.org/10.1016/j.electacta.2007.05.049)
- [13] Rezaei M, Ghorbani M, Dolati A. Electrochemical investigation of electrodeposited Fe–Pd alloy thin films. *Electrochim Acta*, 2010, **56**: 483–490. DOI: [10.1016/j.electacta.2010.09.022](https://doi.org/10.1016/j.electacta.2010.09.022)
- [14] Rao C R K and Trivedi D C. Chemical and electrochemical depositions of platinum group metals and their applications. *Coordin Chem Rev*, 2005, **249**: 613–631. DOI: [10.1016/j.ccr.2004.08.015](https://doi.org/10.1016/j.ccr.2004.08.015)
- [15] McCafferty E. Validation of corrosion rates measured by the Tafel extrapolation method. *Corros Sci*, 2005, **47**: 3202–3215. DOI: [10.1016/j.corsci.2005.05.046](https://doi.org/10.1016/j.corsci.2005.05.046)
- [16] Alvarez A E and Salinas D R. Formation of Cu/Pd bimetallic crystals by electrochemical deposition. *Electrochim Acta*, 2010, **55**: 3714–3720. DOI: [10.1016/j.electacta.2010.01.076](https://doi.org/10.1016/j.electacta.2010.01.076)
- [17] Bard A J and Faulkner L R. *Electrochemical methods-fundamentals of electrochemical analysis*. New York (USA): Ellis Horwood, 1994.